

Small Extracellular Vesicles Derived from Umbilical Cord Mesenchymal Stem Cells Repair Blood-Spinal Cord Barrier Disruption after Spinal Cord Injury through Down-Regulation of Endothelin-1 in Rats

Chenhui Xue¹, Xun Ma^{Corresp., 1, 2}, Xiaoming Guan^{Corresp., 1, 2}, Haoyu Feng^{1, 2}, Mingkui Zheng¹, Xihua Yang³

¹ Third Hospital of Shanxi Medical University, Shanxi Bethune Hospital, Shanxi Academy of Medical Sciences, Tongji Shanxi Hospital, Taiyuan, Shanxi, China

² Department of Orthopedics, Shanxi Bethune Hospital, Shanxi Academy of Medical Sciences, Tongji Shanxi Hospital, Third Hospital of Shanxi Medical University, Taiyuan, Shanxi, China

³ Laboratory Animal Center, Shanxi Province Cancer Hospital/Shanxi Hospital Affiliated to Cancer Hospital, Chinese Academy of Medical Sciences/Cancer Hospital Affiliated to Shanxi Medical University, Taiyuan, Shanxi, China

Corresponding Authors: Xun Ma, Xiaoming Guan

Email address: maxun2532@sina.com, doctor_gxm2012@126.com

Spinal cord injury could cause irreversible neurological dysfunction by destroying the blood-spinal cord barrier (BSCB) and allowing blood cells like neutrophils and macrophages to infiltrate the spinal cord. Small extracellular vesicles (sEVs) derived from mesenchymal stem cells (MSCs) found in the human umbilical cord have emerged as a potential therapeutic alternative to cell-based treatments. This study aimed to investigate the mechanism underlying the alterations in the BSCB permeability by human umbilical cord MSC-derived sEVs (hUC-MSCs-sEVs) after SCI. First, we used hUC-MSCs-sEVs to treat SCI rat models, demonstrating their ability to inhibit BSCB permeability damage, improve neurological repair, and reduce SCI-induced upregulation of prepro-endothelin-1 (prepro-ET-1) mRNA and endothelin-1 (ET-1) peptide expression. Subsequently, we confirmed that hUC-MSCs-sEVs could alleviate cell junction destruction and downregulate MMP-2 and MMP-9 expression after SCI, contributing to BSCB repair through ET-1 inhibition. Finally, we established an in vitro model of BSCB using human brain microvascular endothelial cells and verified that hUC-MSCs-sEVs could increase the expression of junction proteins in endothelial cells after oxygen-glucose deprivation by ET-1 downregulation. This study indicates that hUC-MSCs-sEVs could help maintain BSCB's structural integrity and promote functional recovery by suppressing ET-1 expression.

Small Extracellular Vesicles Derived from Umbilical Cord Mesenchymal Stem Cells Repair Blood-Spinal Cord Barrier Disruption after Spinal Cord Injury through Down-Regulation of Endothelin-1 in Rats

Chenhui Xue¹, Xun Ma^{1,2*}, Xiaoming Guan^{1,2*}, Haoyu Feng^{1,2}, Mingkui Zheng¹, Xihua Yang³

¹ Third Hospital of Shanxi Medical University, Shanxi Bethune Hospital, Shanxi Academy of Medical Sciences, Tongji Shanxi Hospital, Taiyuan, 030032, China

² Department of Orthopedics, Shanxi Bethune Hospital, Shanxi Academy of Medical Sciences, Tongji Shanxi Hospital, Third Hospital of Shanxi Medical University, Taiyuan, 030032, China

³ Laboratory Animal Center, Shanxi Province Cancer Hospital/Shanxi Hospital Affiliated to Cancer Hospital, Chinese Academy of Medical Sciences/Cancer Hospital Affiliated to Shanxi Medical University, 030013, Taiyuan, Shanxi, China

Corresponding Author:

Xun Ma^{1,2}

¹ Third Hospital of Shanxi Medical University, Shanxi Bethune Hospital, Shanxi Academy of Medical Sciences, Tongji Shanxi Hospital, Taiyuan, 030032, China

² Department of Orthopedics, Shanxi Bethune Hospital, Shanxi Academy of Medical Sciences, Tongji Shanxi Hospital, Third Hospital of Shanxi Medical University, Taiyuan, 030032, China

Email address: maxun2532@sina.com

Corresponding Author:

Xiaoming Guan^{1,2}

¹ Third Hospital of Shanxi Medical University, Shanxi Bethune Hospital, Shanxi Academy of Medical Sciences, Tongji Shanxi Hospital, Taiyuan, 030032, China

² Department of Orthopedics, Shanxi Bethune Hospital, Shanxi Academy of Medical Sciences, Tongji Shanxi Hospital, Third Hospital of Shanxi Medical University, Taiyuan, 030032, China

Email address: doctor_gxm2012@126.com

Abstract

Spinal cord injury could cause irreversible neurological dysfunction by destroying the blood-spinal cord barrier (BSCB) and allowing blood cells like neutrophils and macrophages to infiltrate the spinal cord. Small extracellular vesicles (sEVs) derived from mesenchymal stem

39 cells (MSCs) found in the human umbilical cord have emerged as a potential therapeutic
40 alternative to cell-based treatments. This study aimed to investigate the mechanism underlying
41 the alterations in the BSCB permeability by human umbilical cord MSC-derived sEVs (hUC-
42 MSCs-sEVs) after SCI. First, we used hUC-MSCs-sEVs to treat SCI rat models, s demonstrating
43 their ability to inhibit BSCB permeability damage, improve neurological repair, and reduce SCI-
44 induced upregulation of prepro-endothelin-1 (prepro-ET-1) mRNA and endothelin-1 (ET-1)
45 peptide expression. Subsequently, we confirmed that hUC-MSCs-sEVs could alleviate cell
46 junction destruction and downregulate MMP-2 and MMP-9 expression after SCI, contributing to
47 BSCB repair through ET-1 inhibition. Finally, we established an in vitro model of BSCB using
48 human brain microvascular endothelial cells and verified that hUC-MSCs-sEVs could increase
49 the expression of junction proteins in endothelial cells after oxygen-glucose deprivation by ET-1
50 downregulation. This study indicates that hUC-MSCs-sEVs could help maintain BSCB's
51 structural integrity and promote functional recovery by suppressing ET-1 expression.

52

53 Introduction

54 Spinal cord injury (SCI), a central nervous system (CNS) disorder, is characterized by persistent
55 sensory and motor abnormalities. Due to its high morbidity and death, SCI poses a global health
56 burden(Simpson et al., 2012; Ahuja et al., 2017). Injury to neurons and axons directly causes the
57 majority of primary spinal cord injuries, whereas “Spinal cord microenvironment imbalance” is
58 thought to be the cause of secondary spinal cord injury exacerbation(Fan et al., 2018).

59 Restoration of neurological function following SCI is dependent on the integrity of the blood-
60 spinal cord barrier (BSCB), which consists of continuous endothelial cells joined by molecular
61 junctions. The BSCB also serves as a barrier to prevent paracellular and transcellular
62 movement(Jin et al., 2021). Additionally, it may control and limit the entry of outside chemicals
63 into the CNS, maintain the microenvironment's homeostasis, and significantly influence the
64 pathophysiological process of various neurological illnesses(Bartanusz et al., 2011).

65

66 Clinical management for spinal cord injury extends patient lifespan but has limited impact on
67 nerve recovery. And stem cell transplantation is a promising avenue for treating SCI. In this
68 context, human umbilical cord mesenchymal stem cells (hUC-MSCs) have emerged as a
69 promising source of human stem cells for therapeutic interventions due to their widespread
70 availability and minimal ethical concerns(Ullah, Subbarao & Rho, 2015). Transplantation of
71 hUC-MSCs into traumatic spinal cord injuries has shown neuro regenerative properties and
72 improved functional outcomes(Gao et al., 2020). However, similar to other cell-based therapies,
73 hUC-MSC transplantation carries potential risks, including infections, embolism, acute
74 immunogenicity, chronic immunogenicity, and tumorigenicity(Saeedi, Halabian & Imani
75 Fooladi, 2019).

76

77 To address safety concerns associated with the administration of living cells, cell-free therapy
78 has emerged as a compelling alternative. Being acknowledged as vital facilitators of intercellular

79 communication, naturally secreted extracellular vesicles (EVs) possess the innate capacity to
80 stimulate tissue regeneration and, therefore, hold promise as biotherapeutic agents(Kim et al.,
81 2022). sEVs are small EVs ranging from 30 to 100 nm produced by all cells(Zhang et al., 2019).
82 They are essential components of paracrine secretions and mediate cell-to-cell communication
83 by transferring genetic material signals, such as non-coding RNAs and mRNAs, as well as
84 proteins, and inhibiting their degradation(Hessvik & Llorente, 2018). Stem cell-derived sEVs
85 exhibit therapeutic benefits comparable to stem cell transplantation through mechanisms such as
86 anti-apoptosis, immunomodulation, anti-inflammatory effects, and the promotion of
87 angiogenesis(Han et al., 2016).

88

89 In the current context, the restoration of neurological function following spinal cord injury relies
90 on the integrity of the blood-spinal cord barrier (BSCB), although the precise regulatory
91 mechanisms remain unclear. Endothelin (ET) is a potent vasoconstrictor involved in various
92 responses associated with CNS disorders(Leslie et al., 2004),(Hostenbach et al., 2016).
93 Endothelin-1 (ET-1) levels have been found to increase in the cerebrum tissue of traumatic brain
94 injury (TBI) models and spinal cord tissue of SCI models(Maier et al., 2007; A et al., 2019;
95 Michinaga et al., 2020). Overexpression of ET-1 causes loss of endothelial integrity, increases
96 blood-brain barrier permeability, aggravates ischemia and hypoxia, as well as induces tissue
97 necrosis and apoptosis(Peters et al., 2003).

98

99 In summary, SCI presently has limited effective therapeutic options due to its refractory nature.
100 Human umbilical cord mesenchymal stem cell-derived small extracellular vesicles (hUC-MSCs-
101 sEVs) offers a promising approach to SCI treatment(Kang & Guo, 2022). However, their
102 effectiveness and underlying mechanisms remain incompletely understood. Therefore, in this
103 study, we investigated the function of hUC-MSCs-sEVs in BSCB repair after SCI, focusing on
104 the involvement of ET-1.

105

106 **Materials & Methods**

107 **Cell culture**

108 The HUC-MSCs were purchased from Fuyuan Biotechnology (Fuyuan Biotechnology Co., Ltd.
109 Shanghai, CHINA). Cells were cultured in Dulbecco's modified Eagle's medium (DMEM,
110 Gibco, NY, USA) supplemented with 10% fetal bovine serum (FBS, Gibco, NY, USA) and 1%
111 penicillin/streptomycin (Thermo Fisher Scientific, Waltham, MA, USA). Human brain
112 microvascular endothelial cells (HBMECs) were purchased from Meisen Cell Technology
113 (Meisen Cell Technology, Zhejiang, China). Cells were cultured in an endothelial cell medium
114 (ScienCell Research Laboratories, San Diego, CA, USA) and incubated in a humidified
115 atmosphere at 5% CO₂ and 37 °C.

116 **sEVs isolation and characterization**

117 We adhered to the guidelines for the isolation, characterization, and functional analysis of EVs as
118 stipulated in a consensus document published by the International Society of Extracellular
119 Vesicles(Koeppen et al., 2021). Extracellular vesicles were harvested from passage (P) 3 to P5 of
120 the hUC-MSCs. To isolate sEVs, the hUMSC-conditioned medium was first centrifuged at 500 g
121 for 10 minutes to remove cells. Subsequently, the supernatant was centrifuged at 10,000 g for 30
122 minutes to eliminate apoptotic vesicles and other debris. The resulting liquid was then filtered
123 through a 0.22 mm filter. The sEVs were then collected as a pellet using ultracentrifugation
124 (Beckman Optima XPN, 45Ti) at 110,000 g for 70 minutes. The sEVs pellet was resuspended in
125 phosphate-buffered saline (PBS) for purification and subjected to another round of
126 ultracentrifugation at 110,000 g for 70 minutes to remove the contaminating proteins. Finally, the
127 sEVs were resuspended in PBS. The Pierce BCA Protein Assay Kit (Thermo Fisher Scientific,
128 Waltham, MA, USA) was used to assess the protein content of the sEVs. The hUC-MSCs-sEVs
129 sample was stored at -80°C for further analysis. The size of sEVs was determined by
130 nanoparticle tracking analysis (NTA) using ZetaView S/N 17-310 (Particle Metrix, Meerbusch,
131 Germany) along with its associated software. Additionally, transmission electron microscopy
132 (TEM; JEOL Ltd., Tokyo, Japan) was used to morphologically examine isolated sEVs. Western
133 blot analysis was utilized to determine the levels of CD63 (Abcam, Cambridge, UK) and
134 TSG101 (Abcam, Cambridge, UK) in sEVs.

135 **Experimental animals**

136 All animal experimental protocols conformed to the Guide for the Care and Use of Laboratory
137 Animals from the National Institutes of Health (NIH Publications No. 8023), and all procedures
138 were approved by the Shanxi Provincial People's Hospital Institutional Animal Care and Use
139 Committee (Approval No. 2022-089). Adult female Sprague–Dawley rats weighing between 220
140 and 250 g were obtained from the Laboratory Animal Center of Shanxi Cancer Institute (animal
141 production certificate # SCXK (Jin) 2017-0001; Shanxi, China). The entire experimental process
142 was conducted at the same institution (animal usage certificate # SYXK (Jin) 2017-0003; Shanxi,
143 China). Rats were housed in pathogen-free environments, with two to three animals per cage.
144 They were provided with a standard commercial diet, had ad libitum access to water, and
145 maintained under control humidity (40-60%) in a 12-hour light-dark cycle. After the assay, all
146 the surviving animals were euthanized by an intraperitoneal injection of barbiturates at the
147 Laboratory Animal Center of Shanxi Cancer Institute. The rats were randomly assigned to the
148 following four groups: control (n = 20), SCI (n = 20), exo (n = 20), and ET-1 (n = 20) groups.

149 **Spinal cord injury and treatment**

150 Rats were anesthetized with 1% sodium pentobarbital (3 mL/kg, i.p.), and a median dorsal
151 incision was performed at the T10 segment. The surrounding tissues were carefully dissected to
152 expose the T10 vertebral body, spinous process, and spinal cord. The muscles were dissected

153 layer by layer while preserving the integrity of the dura mater. In the sham-operated group, the
154 wound was sutured layer by layer after sterilization. A spinal cord injury model was established
155 using the modified Allen's method for the remaining three groups. The spinal cord injury was
156 created at the T10 level using a standardized force (10 g×5 cm), and the successful modeling was
157 confirmed by the presence of congestion, edema, double hind limb convulsions, and spastic tail
158 swing at the site of injury in the spinal cord.

159 **Treatment**

160 Postoperatively, the ET-1 group was injected 10 μ L (1 μ g/mL) of ET-1 directly into the injured
161 site using a microinjector. The wound was subsequently sutured layer by layer after rinsing with
162 saline and disinfection. The Sham and SCI groups were administered 200 μ L PBS solution in the
163 tail vein immediately after injury and 1 and 2 days post-injury, while 40 μ g sEVs (200 μ g/mL)
164 solution was administered to the sEVs and ET-1 groups. This dosage was chosen based on
165 previous study with sEVs in rats(Zhang et al., 2015). All rats were given intraperitoneal
166 penicillin (200,000 U/d) for 3 days, while their bladder was manually massaged twice or thrice
167 daily to facilitate urination until the urinary function was restored.

168 **Behavioral tests**

169 The Basso, Beattie, and Bresnahan (BBB) ratings were used to assess the functional impairments
170 following SCI. Two independent examiners blinded to the experimental groups evaluated the
171 BBB scores on an open-field scale. Evaluations were performed at 1, 3, 5, 7, 14, and 21 days
172 after surgery to monitor the progression of functional recovery in the rats.

173 **Western blot analysis**

174 For western blot analysis, spinal cord tissue was mixed with RIPA lysate, lysed on ice for 30
175 min, and then centrifuged at 15 000×g for 10 min at 4° C. For protein analysis in vitro,
176 HBMECs were lysed in RIPA buffer with protease and phosphatase inhibitors. The protein
177 content of the supernatants was quantified using the Pierce™ BCA protein assay kit (Thermo
178 Fisher Scientific, Waltham, MA, USA), and the supernatant was collected for subsequent protein
179 analysis. A 10% gel was used to separate equivalent quantities of 20 mg of protein, which were
180 then transferred onto a polyvinylidene difluoride (PVDF) membrane (Merck Millipore,
181 Darmstadt, Germany). Following blocking with 5% nonfat milk in TBS with 0.05% Tween 20
182 for 1 hour, the membrane was incubated with primary antibodies against ZO-1 (61-7300;
183 Thermo Fisher Scientific), beta-catenin (ab32572, Abcam, Cambridge, UK), occluding
184 (ab216327, Abcam), claudin-5 (352500; Santa Cruz Biotechnology, Inc., Dallas, TX, USA),
185 MMP-2 (ab92536, Abcam), and MMP-9 (ab76003, Abcam) at 4°C overnight (around 20 hours).
186 After three TBS-T washes, the membranes were incubated with the secondary antibodies for 1
187 hour at room temperature. The protein bands were visualized using an automated gel imaging
188 system (Bio-Rad ChemiDoc MP, Bio-Rad, Hercules, CA, USA), while the band densities were

189 measured using ImageJ software. The relative density ratios normalized to the Sham or Control
190 group were used to describe the findings.

191 **Real-Time PCR**

192 Spinal cord tissue samples were subjected to isopropanol precipitations after total RNA
193 extraction using the RNAiso plus protocol (TaKaRa Bio Inc., Shiga, Japan). The extracted total
194 RNA was used to synthesize first-strand cDNA. Quantitative reverse transcription-polymerase
195 chain reaction (RT-PCR) was used to measure mRNA levels using SYBR Green fluorescent
196 probes. The SYBR Green Master Mix (TaKaRa Bio Inc., Shiga, Japan) was added to each
197 reverse-transcription product, and the reaction mixture was then subjected to amplification using
198 a CFX96 Touch Real-Time PCR Detection System (Bio-Rad, Hercules, CA, USA).
199 The following primer pairs were used for amplification:

200 Prepro-ET-1 Forward: 5' -GTGAGAACGGCGGGGAGAAAC-3'

201 Reverse: 5' - AATGATGTCCAGGTGGCAGAAGTAG -3'

202 GAPDH: Forward: 5' -CTCTGATTTGGTTCGTATTGGG-3'

203 Reverse: 5' -TGGAAGATGGTGATGGGA TT-3'

204 Serial dilutions of each amplicon were also amplified to generate standard curves for the
205 quantification of the PCR products. The copy numbers of each PCR product, equal to 1 μ g of
206 total RNA, was used to calculate the quantity of mRNA. The prepro-ET-1 mRNA expression
207 levels were normalized to GAPDH values.

208 **Evans Blue Dye Assays**

209 Evans Blue Dye Assays were performed to assess BSCB permeability. A 2% Evans blue saline
210 solution (2 mL/kg) was administered into the tail vein of rats 7 days after SCI. After 2 hours, the
211 rats were anesthetized with 1% sodium pentobarbital (3 mL/kg), and saline was perfused through
212 the heart until clear fluid began to flow from the right atrium. A 1 cm segment of the injured
213 spinal cord, centered around the injury site, was carefully dissected, weighed, and homogenized
214 in a 50% trichloroacetic acid solution. The homogenate was then centrifuged at 10,000 g for 10
215 min, and the supernatant was collected. The absorbance of the sample was measured using a
216 spectrophotometer (with an excitation wavelength of 620 nm and an emission wavelength of 680
217 nm). The established standard curve was used to determine the quantity of Evans dye present in
218 the tissue (μ g/g).

219 **FITC-Dextran Assays**

220 The rats received an intravenous injection of 2% FITC-dextran (MW 70 kDa, 4 mg/kg; Sigma-
221 Aldrich) solution in PBS via the tail vein 1 day after SCI. After 2 hours, the rats were injected
222 with 10% chloral hydrate, followed by perfusion with 0.9% normal saline. The FITC-dextran-
223 damaged spinal cord tissues were weighed, homogenized in PBS, and centrifuged. The optical

224 density of the supernatant was measured using a spectrophotometer at an excitation wavelength
225 of 493 nm and an emission wavelength of 517 nm to assess the presence of FITC-dextran.

226 **Oxygen–glucose deprivation/reoxygenation procedure**

227 Oxygen–glucose deprivation/reoxygenation (OGD/R) procedures were conducted following
228 previously established protocols(Sun et al., 2017). Briefly, cultivated HBMECs were washed
229 thrice with PBS and then transferred to serum-free DMEM without glucose (Gibco, Life
230 Technologies, USA). Subsequently, the HBMECs were subjected to oxygen-glucose deprivation
231 (OGD) by placing them in an anaerobic chamber containing 1% O₂, 5% CO₂, and 94% N₂ at
232 37°C for 6 hours. After being exposed to OGD for 6 hours, the HBMECs were washed once with
233 PBS and then incubated under normal conditions (reoxygenation) for 24 hours.

234 **Cell viability assay**

235 Cell counting kit-8 (CCK-8) assay was used to assess cell viability. HBMECs were cultured in
236 endothelial cell media and seeded in 96-well plates. After 1, 2, 3, 4, and 5 days of incubation, 10
237 μ L of CCK-8 reagent (Dojindo, Japan) was added to the culture medium. A microplate reader
238 (Bio-Rad 680, Hercules, USA) was then used to measure the absorbance of each well at 450 nm.

239 **Paracellular permeability assay**

240 HBMECs were seeded overnight in a 200- μ L medium at a density of 1×10^5 cells/well on
241 Transwell permeable supports (PET membrane 24-well cell culture inserts with 0.4- μ m pore
242 size; Corning; Corning Life Sciences, Corning, NY, USA). Subsequently, the cells were subjected
243 to OGD for 6 hours, followed by reoxygenation for 22 hours (OGD6h/R22h). The cells were
244 then exposed to media containing FITC-dextran (1 mg/ml) for 2 hours. The amount of FITC-
245 dextran passing through the Transwell (in the lower chambers) was determined using an enzyme-
246 labeled meter with an excitation wavelength of 493 nm and an emission wavelength of 517 nm.

247 **Statistical analysis**

248 All the experiments were performed three times at least. All data are shown as mean \pm
249 standard deviation, and statistical analysis was performed in GraphPad Prism (version 8.0,
250 GraphPad Software Inc., USA). One-way ANOVA followed by Tukey's post hoc analysis was
251 used for multiple comparisons. P-value < 0.05 was considered statistically significant.

252

253

254 **Results**

255 **hUC-MSCs-sEVs attenuate SCI-induced BSCB disruption**

256 The successful isolation of the hUC-MSCs-sEVs was confirmed by TEM, which revealed their
257 characteristic cup-shaped morphology (Fig. 1A). The hUC-MSCs-sEVs isolates were further
258 identified using NTA, showing that particles with a diameter of 100 to 140 nm were the
259 predominant populations (Fig. 1B). Western blot analysis of the sEVs lysates demonstrated
260 significant positive bands for CD63 and TSG101, indicating the presence of exosomal markers,
261 while GAPDH was employed as a control for purity (Fig. 1C).

262 The BBB scores were utilized to evaluate the functional recovery. Comparison of locomotor
263 activity between the Exo group and the SCI Group 3–21 days post-injury revealed a remarkable
264 improvement in locomotor function following sEVs therapy (Fig. 1D). Evaluation of BSCB
265 integrity was performed using Evans blue and FITC-dextran fluorescence assays. hUC-MSCs-
266 sEVs significantly reduced the fluorescence intensity of Evans blue in the injured spinal cord
267 (Fig. 1E), and the penetration of FITC-dextran (Fig. 1F). Collectively, these findings
268 demonstrate that hUC-MSCs-sEVs mitigate BSCB disruption in rats after SCI.

269 **hUC-MSCs-sEVs reduce SCI-induced ET-1 expression**

270 Previous studies demonstrated an increase in ET-1 levels in the spinal cord tissue of SCI rats,
271 suggesting that excessive ET-1 production following SCI contributes to vasoconstriction, which
272 is closely associated with spinal cord ischemia and hypoxia symptoms (A et al., 2019). Therefore,
273 we examined the effects of hUC-MSCs-sEVs on SCI-induced ET-1 production. Our results
274 revealed a significant increase in the expression of prepro-ET-1 mRNA and ET-1 peptide
275 following SCI. However, the administration of hUC-MSCs-sEVs at 200 ug/day after SCI
276 reduced the SCI-induced upregulation of prepro-ET-1 mRNA (Fig. 2A) and ET-1 peptide (Fig.
277 2B).

278 **ET-1 is involved in the effects of hUC-MSCs-sEVs on SCI repair**

279 To investigate the role of ET-1 in the cell neurological repair effects of hUC-MSCs-sEVs on the
280 BSCB after SCI, ET-1 was administered at the injury site after SCI. Our results demonstrated
281 that ET-1 injection significantly reduced the therapeutic effect of sEVs on motor activity 3-21
282 days post-SCI (Figure 3A). Furthermore, at 24 hours following SCI, Evans blue dye
283 extravasation was assessed. The findings of the Evans blue dye (Fig. 3B) and Evans blue
284 extravasation tests (Fig. 3C) revealed that ET-1 reversed the protective effect conferred by hUC-
285 MSCs-sEVs. Additionally, FITC-dextran penetration, which was decreased by the administration
286 of hUC-MSCs-sEVs, was significantly increased following ET-1 injection (Fig. 3D). According
287 to the aforementioned data, hUC-MSCs-sEVs enhances functional recovery and lessens BSCB
288 disruption following SCI via ET-1.

289 **hUC-MSCs-sEVs increase the expression of junction proteins after SCI by**
290 **downregulation of ET-1**

291 We performed a Western blot analysis to examine whether hUC-MSCs-sEVs can protect the
292 integrity of the BSCB by regulating tight junction proteins and adhesion junction proteins. Our
293 results demonstrated a significant reduction in the expression levels of ZO-1, β -catenin, occludin,
294 and claudin-5 following SCI. However, treatment with hUC-MSCs-sEVs attenuated these
295 changes, thereby promoting the restoration of BSCB integrity. Notably, the therapeutic effect of
296 sEVs was also significantly compromised upon ET-1 injection (Fig. 4A-4E). According to the
297 aforementioned data, hUC-MSCs-sEVs enhances expression of cell junction proteins following
298 SCI via downregulation of ET-1.

299 **hUC-MSCs-sEVs decreases expression of inflammatory mediators in SCI rats by**
300 **downregulation of ET-1**

301 Previous studies have highlighted the crucial role of matrix metalloproteinase (MMP) in the
302 recovery process following SCI (Yu et al., 2008). Notably, MMP-2 and MMP-9 are known to be
303 modulated by ET-1 (He, Prasanna & Yorio, 2007; Wang et al., 2010). Therefore, we
304 subsequently evaluated the levels of MMP-2 and MMP-9 to confirm that the impact of hUC-
305 MSCs-sEVs therapy in SCI rats was caused by the reduced expression of ET-1. Western blot
306 analysis revealed significantly elevated expression levels of MMP-2 and MMP-9 in SCI rats
307 compared to the Sham group. However, the administration of hUC-MSCs-sEVs resulted in a
308 significant decrease in MMP-2 and MMP-9 expression. The therapeutic effect of sEVs was
309 reduced upon ET-1 injection (Fig. 5A-5C).

310 **hUC-MSCs-sEVs increase the expression of junction proteins in HBMECs after**
311 **OGD/R by downregulation of ET-1**

312 To detect the effects of hUC-MSCs-sEVs on OGD/R-injured HBMECs, we conducted a series of
313 experiments, including Western blot analysis, Cell Viability Assay, and Paracellular
314 Permeability Assay. The expressions of junctional proteins, including Claudin-5, Occludin, beta-
315 Catenin, and ZO-1, were significantly decreased in HBMECs subjected to OGD/R. However, the
316 presence of hUC-MSCs-sEVs notably reversed this decrease in expression, and this therapeutic
317 effect was reduced upon ET-1 administration (Fig. 6A-E). Moreover, we detected that hUC-
318 MSCs-sEVs significantly enhanced cell viability, whereas ET-1 exerted an inhibitory effect (Fig.
319 6F). To investigate the impact of OGD/R and ET-1 on the integrity of HBMECs, FITC-dextran
320 was added to the cells. Our results confirmed that OGD/R significantly increased cell
321 permeability, while hUC-MSCs-sEVs addition significantly attenuated this effect. Interestingly,
322 the introduction of ET-1 significantly increased endothelial barrier permeability (Fig. 6G).

323

324 **Discussion**

325 In this study, we demonstrated that hUC-MSCs-sEVs mitigate neurological impairments by

326 preserving the integrity of the BSCB in SCI-affected rats. We demonstrated that hUC-MSCs-
327 sEVs suppress ET-1 expression, thereby preventing the disruption of cell junctions following
328 SCI, facilitating BSCB repair. Our study sheds light on the underlying mechanism through which
329 hUC-MSCs-sEVs exert their influence on BSCB integrity after SCI.

330

331 Growing evidence indicates that the BSCB may be indispensable to the pathophysiology of
332 SCI(Jin et al., 2021). This barrier maintains the homeostasis of the spinal cord by regulating
333 molecular exchanges between blood vessels and spinal parenchyma(Abbott et al., 2010).
334 However, in clinical settings and animal models, SCI often leads to BSCB destruction, resulting
335 in morphological and functional changes, such as vascular alterations, increased permeability,
336 spinal cord edema, and spinal cord cavity formation(Jin et al., 2021)⁵. Mesenchymal stem cells
337 derived sEVs have been shown to impact various processes, such as neuronal apoptosis,
338 angiogenesis, and inflammation in SCI.(Liu et al., 2019) However, their role in BSCB repair
339 remains an ongoing investigation. In our current study, we performed various assays for BSCB
340 permeability, such as Evans Blue Dye Assays, FITC-Dextran Assays, and Paracellular
341 Permeability Assay, in SCI-model rats, with or without sEVs treatment. Our findings
342 demonstrate that hUC-MSCs-sEVs effectively reduce neurological impairments by preserving
343 the integrity of the BSCB in rats with SCI.

344

345 Tight junctions between individual endothelial cells highly regulate the paracellular diffusion
346 pathway in brain capillary endothelial cells(Abbott et al., 2010). Among the plasma membrane
347 proteins responsible for the formation of tight junctions are claudin, occludin, and adherens
348 junction molecules. The zonula occludens protein and cingulin form the cytoplasmic components
349 of tight junctions(Abbott, Rönnbäck & Hansson, 2006; Bernacki et al., 2008). We examined tight
350 junction membrane proteins and cytoplasmic components, such as claudin-5, Occluding, β -
351 Catenin, and ZO-1, using Western blot analysis. Our results confirmed that hUC-MSCs-sEVs
352 regulate the expression of tight junction proteins, thereby alleviating BSCB disruption after SCI.

353

354 Matrix metalloproteinases (MMPs) are a family of zinc-containing peptidases secreted by
355 neutrophils. These peptidases destroy and restructure the extracellular matrix as well as other
356 extracellular proteins. Matrix metalloproteinases are an essential component of barrier
357 function(Beck et al., 2010). MMPs could instantly infiltrate the parenchyma of the spinal cord
358 following the injury and continue to reside at the lesion site for more than 10 days(Carlson et al.,
359 1998). MMPs, particularly MMP-2 and MMP-9, are prominently expressed 7 days after SCI and
360 contribute to BSCB breakdown under pathological conditions(Yao et al., 2018; Wang et al.,
361 2021). Our study also revealed elevated expression of MMP-2 and MMP-9 in the spinal cord
362 tissue of rats after SCI. Administration of hUC-MSCs-sEVs decreased the expression of MMP-2
363 and MMP-9, indicating that hUC-MSCs-sEVs could mitigate BSCB disruption mediated by
364 these MMPs. Our findings also provide further insight into the molecular mechanisms
365 underlying the protective effects of sEVs on BSCB disruption after SCI.

366

367 Notably, our results show that the beneficial effects of hUC-MSCs-sEVs on SCI were
368 significantly inhibited in the presence of ET-1, a vasoconstrictive peptide composed of 21 amino
369 acids. Increased expression of ET-1 has been correlated with the pattern of BSCB degradation
370 after SCI. Pharmacological blockade of ET-1-mediated vasoconstriction has been shown to
371 attenuate BSCB degradation after SCI.(McKenzie et al., 1995) And intrathecal administration of
372 ET-1 in the intact spinal cord resulted in disruption of the BSCB.(Westmark et al., 1995) In this
373 study, ET-1 injection in the wound site significantly reduced the therapeutic effects of hUC-
374 MSCs-sEVs. *In vitro* experiments further demonstrated that hUC-MSCs-sEVs increased the
375 expression of tight junction and adhesion junction proteins, enhanced cell viability, and
376 decreased cell permeability following OGD/R. Furthermore, the administration of ET-1 to
377 HBMECs led to corresponding changes in the expression of tight junction proteins, adhesion
378 junction proteins, cell viability, and permeability. These findings confirm that the regulatory
379 effect of hUC-MSCs-sEVs on BSCB function is mediated through the modulation of ET-1
380 expression.

381

382 It should be noted that there are some limitations to this study. First, sEVs consist of a class of
383 nanovesicles that contain various substances derived from parental cells, such as miRNA,
384 mRNA, and protein, and transport them to recipient cells (Kalluri and LeBleu, 2020). Exactly
385 which of these components exerted a role in regulating ET-1 and ameliorating BSCB destruction
386 was not investigated in this study. These functional components need to be further identified in
387 subsequent studies. Second, the spinal cord has a variety of cell types, each of which performs a
388 distinctive function and interacts with others in the destruction of the BSCB after SCI. Due of
389 this, microglia and astrocytes both contribute significantly to the development of BSCB
390 destruction following SCI. In the current investigation, we only looked at how sEVs affected
391 endothelial cells. It is important to carry out additional *in vitro* and *in vivo* research using co-
392 culture systems with mixed endothelial cells and other spinal cord cell types. Third, the current
393 study did not examine ET-1 receptors ETaR and ETbR or additional signalling pathways that are
394 involved in ET-1 intracellular signalling. Future research will need to focus on these receptors
395 and signalling pathways. Forth, only female rats were chosen for this study, because they are
396 more commonly used in current spinal cord injury research and they exhibit less fighting
397 behavior compared to males, which facilitates comparisons and references to previous studies
398 and improves the stability of experimental results(Cheng et al., 2012; Torres-Espín et al., 2018;
399 Vawda et al., 2019). In our future research, we consider including male models to obtain a more
400 comprehensive understanding of the regulatory mechanisms of the therapeutic effects of hUC-
401 MSCs-sEVs on SCI.

402

403

404 **Conclusions**

405 In conclusion, the current study provides evidence for the protective effect of hUC-MSCs-sEVs
406 on BSCB integrity following SCI. We demonstrate that hUC-MSCs-sEVs attenuate BSCB
407 degradation and promote functional recovery after SCI by regulating the expression of ET-1. We
408 further elucidate the mechanism by which hUC-MSCs-sEVs exert their influence on BSCB
409 integrity after SCI.

410
411

412 **Acknowledgements**

413 We would like to thank the Shanxi Provincial Key Laboratory of Kidney Disease, the Core
414 Laboratory at Shanxi Provincial People's Hospital and the Laboratory Animal Center at Shanxi
415 Province Cancer Hospital for their technical support.

416 We thank Bullet Edits Limited for the linguistic editing and proofreading of the manuscript.

417
418

419 **References**

- 420 A J-C, Li Z-Y, Long Q-F, Wang D-Y, Zhao H-S, Jia S-L, Zhang W-H. 2019. MiR-379-5p
421 improved locomotor function recovery after spinal cord injury in rats by reducing endothelin 1
422 and inhibiting astrocytes expression. *European Review for Medical and Pharmacological*
423 *Sciences* 23:9738–9745. DOI: 10.26355/eurrev_201911_19536.
- 424 Abbott NJ, Patabendige AAK, Dolman DEM, Yusof SR, Begley DJ. 2010. Structure and
425 function of the blood-brain barrier. *Neurobiology of Disease* 37:13–25. DOI:
426 10.1016/j.nbd.2009.07.030.
- 427 Abbott NJ, Rönnbäck L, Hansson E. 2006. Astrocyte-endothelial interactions at the blood-brain
428 barrier. *Nature Reviews. Neuroscience* 7:41–53. DOI: 10.1038/nrn1824.
- 429 Ahuja CS, Wilson JR, Nori S, Kotter MRN, Druschel C, Curt A, Fehlings MG. 2017. Traumatic
430 spinal cord injury. *Nature Reviews. Disease Primers* 3:17018. DOI: 10.1038/nrdp.2017.18.
- 431 Bartanusz V, Jezova D, Alajajian B, Digicaylioglu M. 2011. The blood-spinal cord barrier:
432 morphology and clinical implications. *Annals of Neurology* 70:194–206. DOI:
433 10.1002/ana.22421.
- 434 Beck KD, Nguyen HX, Galvan MD, Salazar DL, Woodruff TM, Anderson AJ. 2010.
435 Quantitative analysis of cellular inflammation after traumatic spinal cord injury: evidence for a
436 multiphasic inflammatory response in the acute to chronic environment. *Brain: A Journal of*
437 *Neurology* 133:433–447. DOI: 10.1093/brain/awp322.
- 438 Bernacki J, Dobrowolska A, Nierwińska K, Małecki A. 2008. Physiology and pharmacological
439 role of the blood-brain barrier. *Pharmacological reports: PR* 60:600–622.
- 440 Carlson SL, Parrish ME, Springer JE, Doty K, Dossett L. 1998. Acute inflammatory response in
441 spinal cord following impact injury. *Experimental Neurology* 151:77–88. DOI:
442 10.1006/exnr.1998.6785.
- 443 Cheng I, Mayle RE, Cox CA, Park DY, Smith RL, Corcoran-Schwartz I, Ponnusamy KE,
444 Oshtory R, Smuck MW, Mitra R, Kharazi AI, Carragee EJ. 2012. Functional assessment of the

- 445 acute local and distal transplantation of human neural stem cells after spinal cord injury. *The*
446 *Spine Journal* 12:1040–1044. DOI: 10.1016/j.spinee.2012.09.005.
- 447 Fan B, Wei Z, Yao X, Shi G, Cheng X, Zhou X, Zhou H, Ning G, Kong X, Feng S. 2018.
448 Microenvironment Imbalance of Spinal Cord Injury. *Cell Transplantation* 27:853–866. DOI:
449 10.1177/0963689718755778.
- 450 Gao L, Peng Y, Xu W, He P, Li T, Lu X, Chen G. 2020. Progress in Stem Cell Therapy for
451 Spinal Cord Injury. *Stem Cells International* 2020:2853650. DOI: 10.1155/2020/2853650.
- 452 Han C, Sun X, Liu L, Jiang H, Shen Y, Xu X, Li J, Zhang G, Huang J, Lin Z, Xiong N, Wang T.
453 2016. Exosomes and Their Therapeutic Potentials of Stem Cells. *Stem Cells International*
454 2016:7653489. DOI: 10.1155/2016/7653489.
- 455 He S, Prasanna G, Yorio T. 2007. Endothelin-1-mediated signaling in the expression of matrix
456 metalloproteinases and tissue inhibitors of metalloproteinases in astrocytes. *Investigative*
457 *Ophthalmology & Visual Science* 48:3737–3745. DOI: 10.1167/iovs.06-1138.
- 458 Hessvik NP, Llorente A. 2018. Current knowledge on exosome biogenesis and release. *Cellular*
459 *and molecular life sciences: CMLS* 75:193–208. DOI: 10.1007/s00018-017-2595-9.
- 460 Hostenbach S, D’haeseleer M, Kooijman R, De Keyser J. 2016. The pathophysiological role of
461 astrocytic endothelin-1. *Progress in Neurobiology* 144:88–102. DOI:
462 10.1016/j.pneurobio.2016.04.009.
- 463 Jin L-Y, Li J, Wang K-F, Xia W-W, Zhu Z-Q, Wang C-R, Li X-F, Liu H-Y. 2021. Blood-Spinal
464 Cord Barrier in Spinal Cord Injury: A Review. *Journal of Neurotrauma* 38:1203–1224. DOI:
465 10.1089/neu.2020.7413.
- 466 Kang J, Guo Y. 2022. Human Umbilical Cord Mesenchymal Stem Cells Derived Exosomes
467 Promote Neurological Function Recovery in a Rat Spinal Cord Injury Model. *Neurochemical*
468 *Research* 47:1532–1540. DOI: 10.1007/s11064-022-03545-9.
- 469 Kim HY, Kwon S, Um W, Shin S, Kim CH, Park JH, Kim B. 2022. Functional Extracellular
470 Vesicles for Regenerative Medicine. *Small* 18:2106569. DOI: 10.1002/smll.202106569.
- 471 Koeppe K, Nymon A, Barnaby R, Li Z, Hampton TH, Ashare A, Stanton BA. 2021. CF
472 monocyte-derived macrophages have an attenuated response to extracellular vesicles secreted by
473 airway epithelial cells. *American Journal of Physiology-Lung Cellular and Molecular*
474 *Physiology* 320:L530–L544. DOI: 10.1152/ajplung.00621.2020.
- 475 Leslie SJ, Rahman MQ, Denvir MA, Newby DE, Webb DJ. 2004. Endothelins and their
476 inhibition in the human skin microcirculation: ET[1-31], a new vasoconstrictor peptide. *British*
477 *Journal of Clinical Pharmacology* 57:720–725. DOI: 10.1111/j.1365-2125.2004.02074.x.
- 478 Liu W, Wang Y, Gong F, Rong Y, Luo Y, Tang P, Zhou Z, Zhou Z, Xu T, Jiang T, Yang S, Yin
479 G, Chen J, Fan J, Cai W. 2019. Exosomes Derived from Bone Mesenchymal Stem Cells Repair
480 Traumatic Spinal Cord Injury by Suppressing the Activation of A1 Neurotoxic Reactive
481 Astrocytes. *Journal of Neurotrauma* 36:469–484. DOI: 10.1089/neu.2018.5835.
- 482 Maier B, Lehnert M, Laurer HL, Marzi I. 2007. Biphasic elevation in cerebrospinal fluid and
483 plasma concentrations of endothelin 1 after traumatic brain injury in human patients. *Shock*
484 (*Augusta, Ga.*) 27:610–614. DOI: 10.1097/shk.0b013e31802f9eaf.

- 485 McKenzie AL, Hall JJ, Aihara N, Fukuda K, Noble LJ. 1995. Immunolocalization of endothelin
486 in the traumatized spinal cord: relationship to blood-spinal cord barrier breakdown. *Journal of*
487 *Neurotrauma* 12:257–268. DOI: 10.1089/neu.1995.12.257.
- 488 Michinaga S, Inoue A, Yamamoto H, Ryu R, Inoue A, Mizuguchi H, Koyama Y. 2020.
489 Endothelin receptor antagonists alleviate blood-brain barrier disruption and cerebral edema in a
490 mouse model of traumatic brain injury: A comparison between bosentan and ambrisentan.
491 *Neuropharmacology* 175:108182. DOI: 10.1016/j.neuropharm.2020.108182.
- 492 Peters CM, Rogers SD, Pomonis JD, Egnaczyk GF, Keyser CP, Schmidt JA, Ghilardi JR,
493 Maggio JE, Mantyh PW. 2003. Endothelin receptor expression in the normal and injured spinal
494 cord: potential involvement in injury-induced ischemia and gliosis. *Experimental Neurology*
495 180:1–13. DOI: 10.1016/s0014-4886(02)00023-7.
- 496 Saeedi P, Halabian R, Imani Fooladi AA. 2019. A revealing review of mesenchymal stem cells
497 therapy, clinical perspectives and Modification strategies. *Stem Cell Investigation* 6:34. DOI:
498 10.21037/sci.2019.08.11.
- 499 Simpson LA, Eng JJ, Hsieh JTC, Wolfe DL, Spinal Cord Injury Rehabilitation Evidence Scire
500 Research Team. 2012. The health and life priorities of individuals with spinal cord injury: a
501 systematic review. *Journal of Neurotrauma* 29:1548–1555. DOI: 10.1089/neu.2011.2226.
- 502 Sun L, Li M, Ma X, Feng H, Song J, Lv C, He Y. 2017. Inhibition of HMGB1 reduces rat spinal
503 cord astrocytic swelling and AQP4 expression after oxygen-glucose deprivation and
504 reoxygenation via TLR4 and NF- κ B signaling in an IL-6-dependent manner. *Journal of*
505 *Neuroinflammation* 14:231. DOI: 10.1186/s12974-017-1008-1.
- 506 Torres-Espín A, Forero J, Fenrich KK, Lucas-Osma AM, Krajacic A, Schmidt E, Vavrek R,
507 Raposo P, Bennett DJ, Popovich PG, Fouad K. 2018. Eliciting inflammation enables successful
508 rehabilitative training in chronic spinal cord injury. *Brain* 141:1946–1962. DOI:
509 10.1093/brain/awy128.
- 510 Ullah I, Subbarao RB, Rho GJ. 2015. Human mesenchymal stem cells - current trends and future
511 prospective. *Bioscience Reports* 35:e00191. DOI: 10.1042/BSR20150025.
- 512 Vawda R, Badner A, Hong J, Mikhail M, Lakhani A, Dragas R, Xhima K, Barretto T, Librach
513 CL, Fehlings MG. 2019. Early Intravenous Infusion of Mesenchymal Stromal Cells Exerts a
514 Tissue Source Age-Dependent Beneficial Effect on Neurovascular Integrity and Neurobehavioral
515 Recovery After Traumatic Cervical Spinal Cord Injury. *Stem Cells Translational Medicine*
516 8:639–649. DOI: 10.1002/sctm.18-0192.
- 517 Wang H-H, Hsieh H-L, Wu C-Y, Yang C-M. 2010. Endothelin-1 enhances cell migration via
518 matrix metalloproteinase-9 up-regulation in brain astrocytes. *Journal of Neurochemistry*
519 113:1133–1149. DOI: 10.1111/j.1471-4159.2010.06680.x.
- 520 Wang X, Shi Q, Ding J, Liang J, Lin F, Cai B, Chen Y, Zhang G, Xu J, Lian X. 2021. Human
521 Bone Marrow Mesenchymal Stem Cell-Derived Exosomes Attenuate Blood-Spinal Cord Barrier
522 Disruption via the TIMP2/MMP Pathway After Acute Spinal Cord Injury. *Molecular*
523 *Neurobiology* 58:6490–6504. DOI: 10.1007/s12035-021-02565-w.

- 524 Westmark R, Noble LJ, Fukuda K, Aihara N, McKenzie AL. 1995. Intrathecal administration of
525 endothelin-1 in the rat: impact on spinal cord blood flow and the blood-spinal cord barrier.
526 *Neuroscience Letters* 192:173–176. DOI: 10.1016/0304-3940(95)11638-d.
- 527 Yao Y, Xu J, Yu T, Chen Z, Xiao Z, Wang J, Hu Y, Wu Y, Zhu D. 2018. Flufenamic acid
528 inhibits secondary hemorrhage and BSCB disruption after spinal cord injury. *Theranostics*
529 8:4181–4198. DOI: 10.7150/thno.25707.
- 530 Yu F, Kamada H, Niizuma K, Endo H, Chan PH. 2008. Induction of mmp-9 expression and
531 endothelial injury by oxidative stress after spinal cord injury. *Journal of Neurotrauma* 25:184–
532 195. DOI: 10.1089/neu.2007.0438.
- 533 Zhang Y, Chopp M, Meng Y, Katakowski M, Xin H, Mahmood A, Xiong Y. 2015. Effect of
534 exosomes derived from multipotent mesenchymal stromal cells on functional recovery and
535 neurovascular plasticity in rats after traumatic brain injury. *Journal of Neurosurgery* 122:856–
536 867. DOI: 10.3171/2014.11.JNS14770.
- 537 Zhang Y, Liu Y, Liu H, Tang WH. 2019. Exosomes: biogenesis, biologic function and clinical
538 potential. *Cell & Bioscience* 9:19. DOI: 10.1186/s13578-019-0282-2.
- 539

Figure 1

hUC-MSCs-sEVs attenuate SCI-induced BSCB disruption.

(A) TEM photomicrographs of hUC-MSCs-s ; scale bar = 200nm. (B) NTA results of hUC-MSCs-s . (C) Western blotting showed the presence of exosomal markers, including CD63, and TSG101, in hUC-MSCs-s . (D) The BBB scores. *P < 0.05 versus the Sham group; **P < 0.01 versus sham-operated group; n = 3. (E) Quantification of the amount of Evans Blue at 7day ($\mu\text{g/g}$). (F) FITC-dextran was used in the spinal cord peripheral penetration analysis results at 7day.

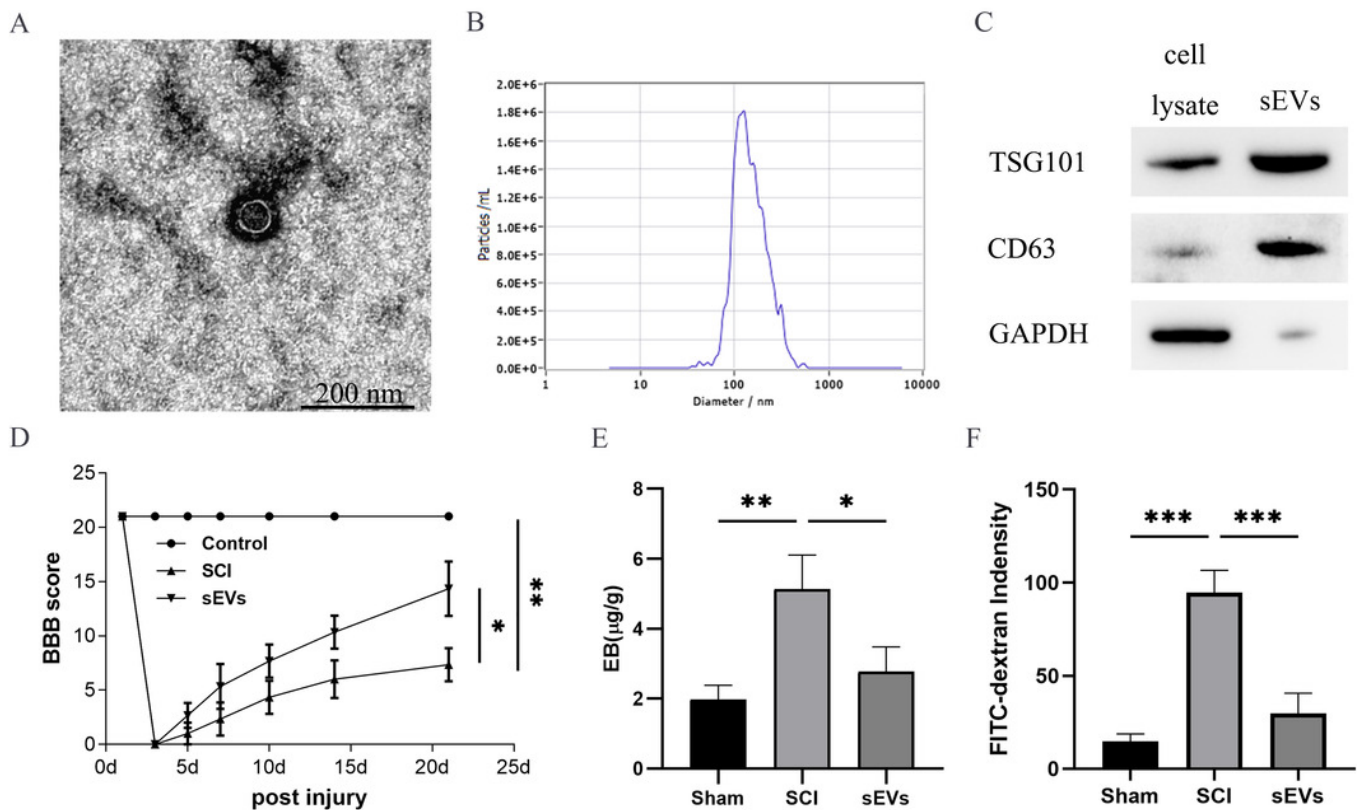


Figure 2

hUC-MSCs-sEVs increase SCI-induced ET-1 production.

(A) Increased prepro- ET-1 mRNA after SCI. Expression levels of prepro- ET-1 mRNA in rat spinal cord tissue were measured at 1 days after SCI. Expression levels of prepro- ET-1 mRNA were normalized to GAPDH. Results represent mean \pm SEM. * $P < 0.05$ versus the Sham group; ** $P < 0.01$ versus sham-operated group; $n = 3$. (B) Increased ET-1 peptide after SCI. Production of ET-1 peptide in the spinal cord tissue was measured by ELISA at 1 days after SCI. The experiments were replicated three times. Results represent mean \pm SEM, with experimental data shown as ET-1 peptide content (ng) per spinal cord tissue weight (g). * $P < 0.05$ versus sham-operated group; $n = 3$.

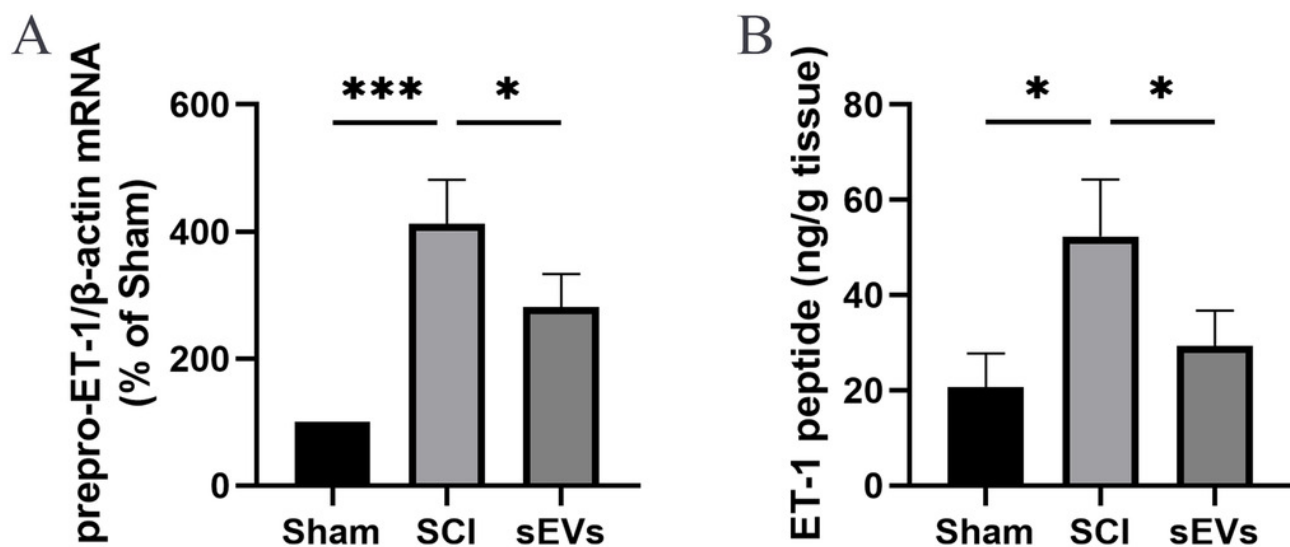


Figure 3

ET-1 is involved in the effects of hUC-MSCs-s EVs on SCI repair.

(A) The BBB scores. ****P < 0.0001 versus the Sham group; n = 3. (B) Representative spinal cords show that Evans Blue dye permeabilized the injured spinal cord at 7 day; scale bar = 3mm. (C) Quantification of the amount of Evans Blue at 7day ($\mu\text{g/g}$). *P < 0.05 versus the Sham group; **P < 0.01 versus the Sham group; ***P < 0.001 versus the Sham group; n = 3. (D) FITC-dextran was used in the spinal cord peripheral penetration analysis results at 7day. The experiments were replicated three times. ***P < 0.001 versus the Sham group; ****P < 0.0001 versus the Sham group; n = 3.

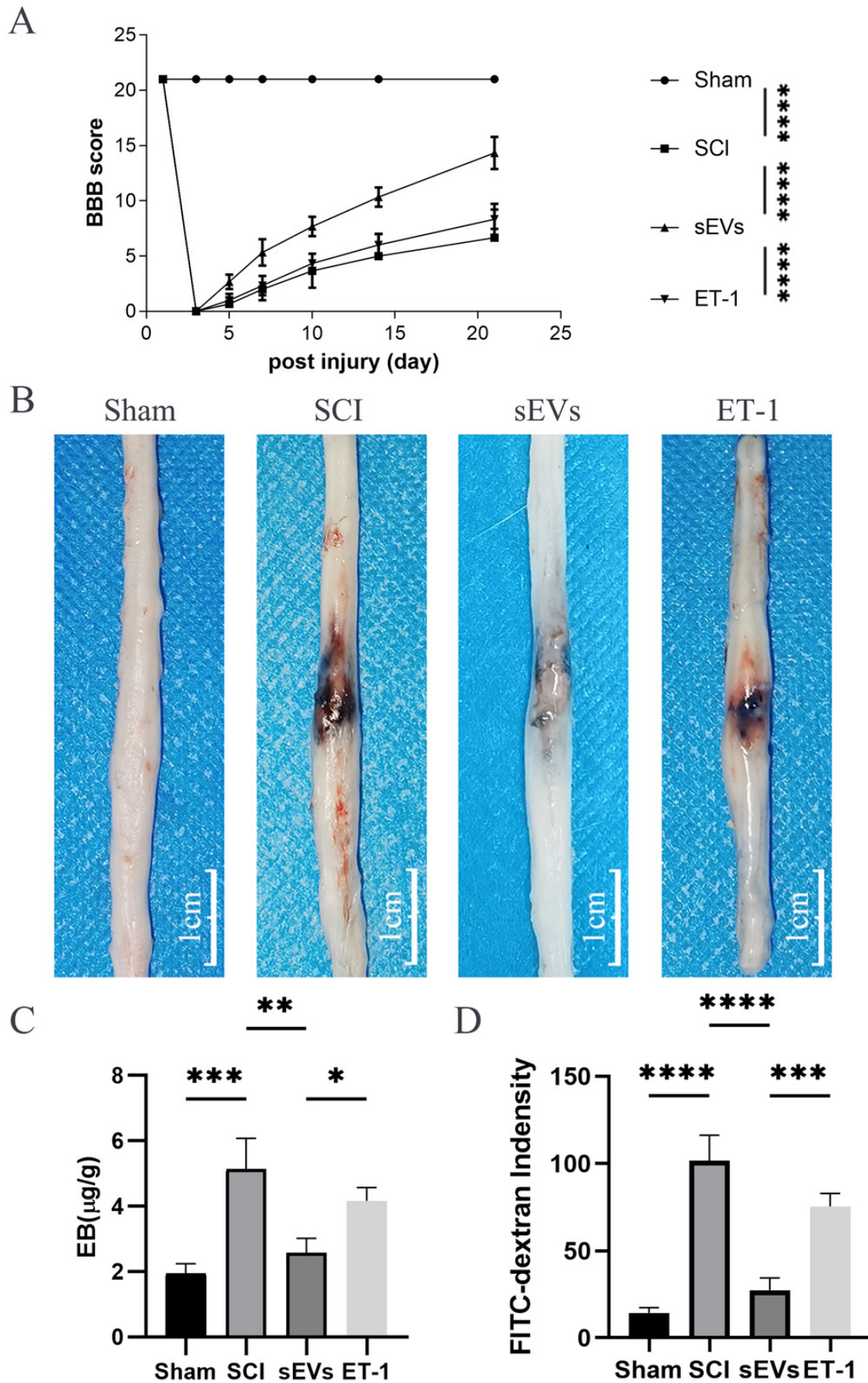


Figure 4

hUC-MSCs-s EVs Increase the Expression of Junction Proteins After SCI by Down-Regulation of ET-1 .

(A-E) Western blot analysis of zo-1, β -catenin, occludin, and claudin-5 in the spinal cord of the sham, SCI, s EVs , and ET-1 groups 1day after SCI. The experiments were replicated three times. **P < 0.01 versus the sham group; ***P < 0.001 versus the Sham group; ****P < 0.0001 versus the Sham group; n = 3.

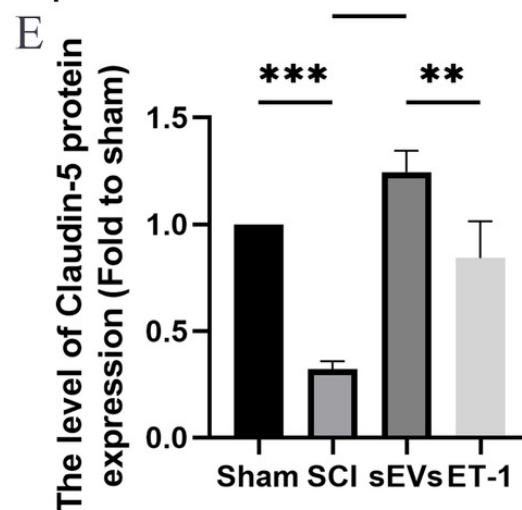
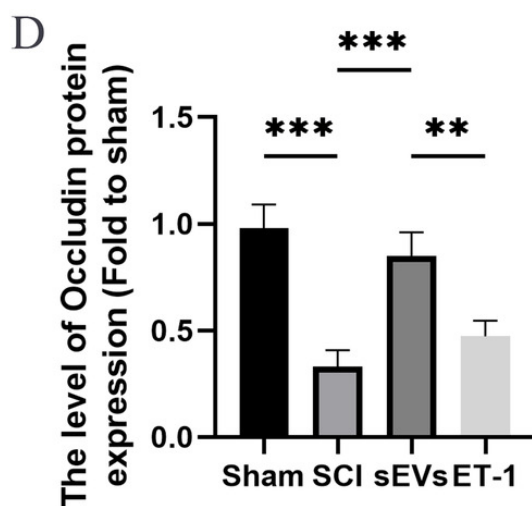
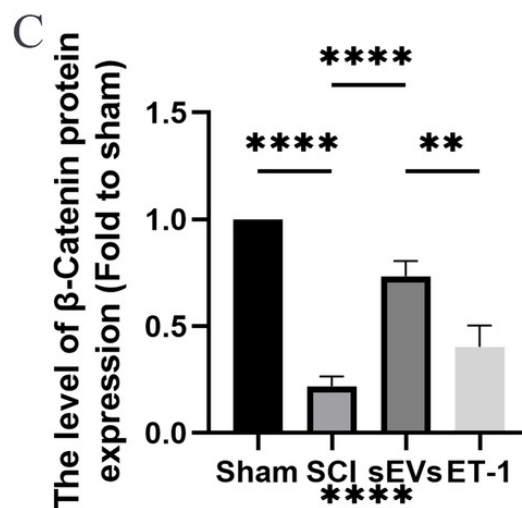
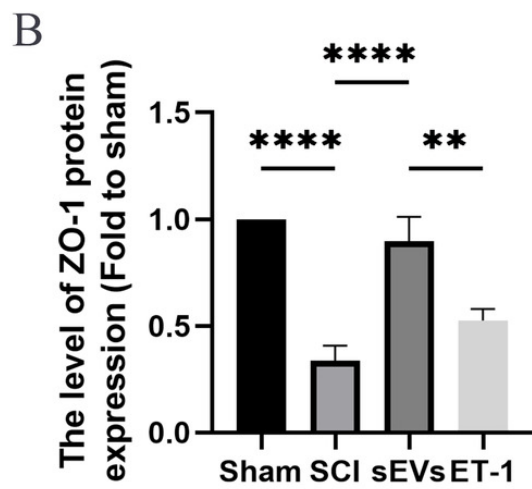
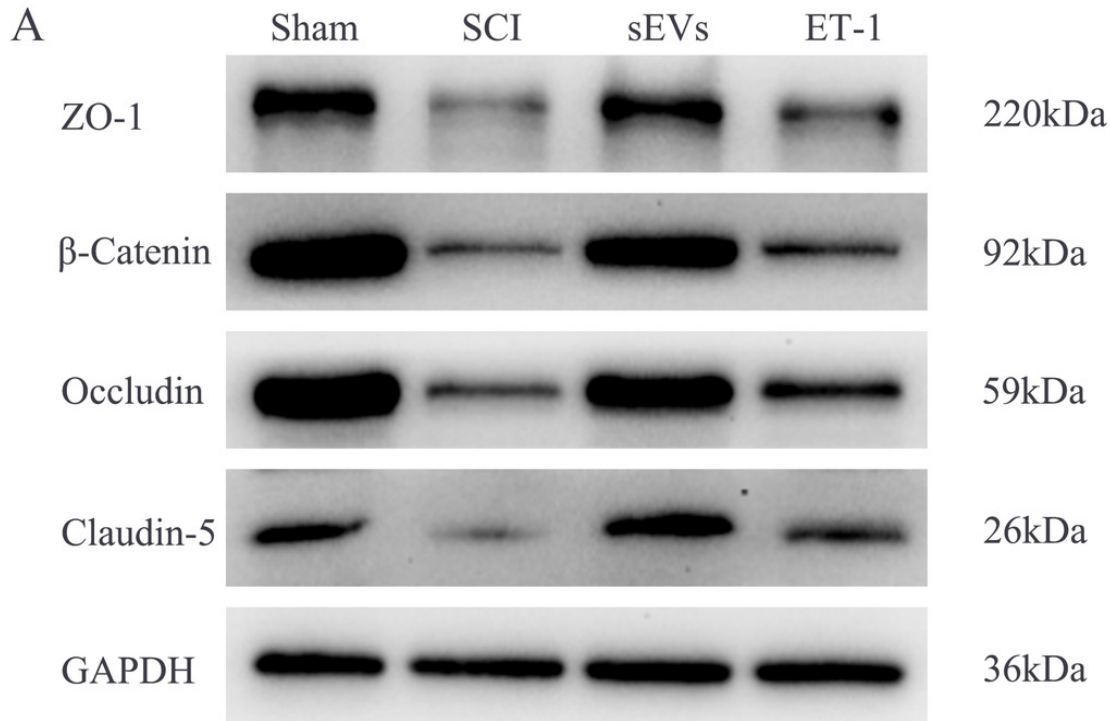


Figure 5

hUC-MSCs-s EVs decreases expression of inflammatory mediators in SCI rats by Down-Regulation of ET-1 .

(A-C) Western blot analysis of MMP-2, and MMP-9 in the spinal cord of the sham, SCI, s EVs , and ET-1 groups 1day after SCI. The experiments were replicated three times. *P < 0.05 versus the Sham group; **P < 0.01 versus the sham group; ***P < 0.001 versus the Sham group; n = 3.

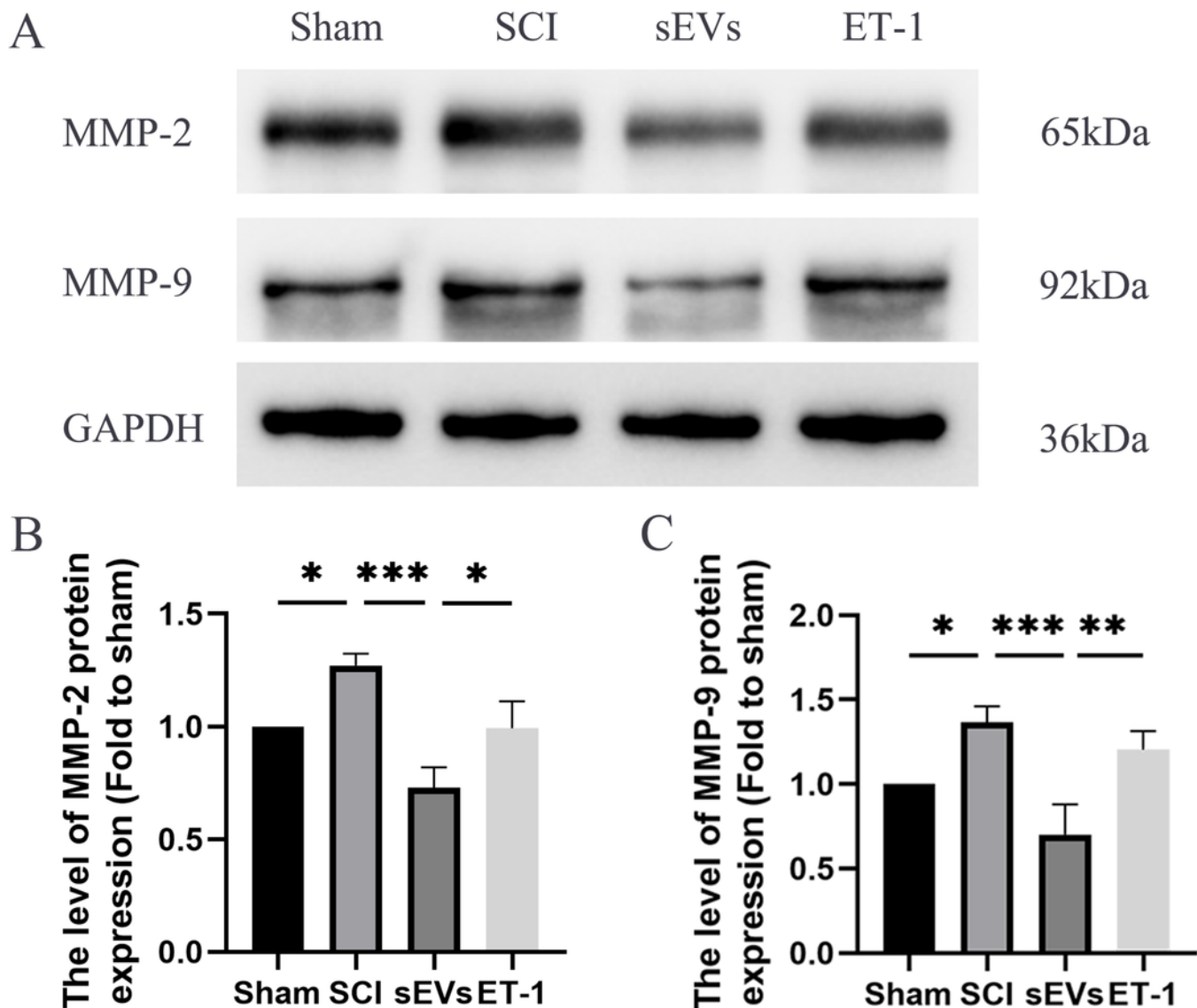


Figure 6

hUC-MSCs-s EVs Increase the Expression of Junction Proteins in endothelial cells after OGD/R by Down-Regulation of ET-1 .

(A-E) Western blot analysis of zo-1, β -catenin, occludin, and claudin-5 in the HBMECs of the Control, OGD/R, s EVs , and ET-1 groups. *P < 0.05 versus the Control group; **P < 0.01 versus the Control group; ***P < 0.001 versus the Control group; ****P < 0.0001 versus the Control group; n = 3. (F) The viability of HBMECs of the Control, OGD/R, s EVs , and ET-1 groups was tested by CCK-8 analysis. The experiments were replicated three times. *P < 0.05 versus the Control group; ****P < 0.0001 versus the Control group; n = 3. (G) Under different conditions, FITC-dextran permeates the fluorescence intensity of the lower chamber. *P < 0.05 versus the Control group; ***P < 0.001 versus the Control group; n = 3.

